Water Research 186 (2020) 116357

Contents lists available at ScienceDirect

Water Research

journal homepage: www.elsevier.com/locate/watres

Bacterially assembled biopolyester nanobeads for removing cadmium from water

Catarina R. Marques[a,*], David Wibowo[b], Patricia Rubio-Reyes[c], Luísa S. Serafim[d], Amadeu M.V.M. Soares[a], Bernd H.A. Rehm[b]

[a] CESAM - Centre of Marine and Environmental Studies, Department of Biology, University of Aveiro, Santiago University Campus, 3810-193 Aveiro, Portugal
[b] Centre for Cell Factories and Biopolymers, Griffith Institute for Drug Discovery, Griffith University, Nathan, QLD 4111, Australia
[c] Malaghan Institute of Medical Research, Gate 7, Victoria University Central Services Building, Kelburn, Wellington 6012, New Zealand
[d] CICECO – Aveiro Institute of Materials, Chemistry Department, University of Aveiro, 3810-193 Aveiro, Portugal

ARTICLE INFO

Article history:
Received 1 June 2020
Revised 24 August 2020
Accepted 29 August 2020
Available online 29 August 2020

Keywords:
Cadmium
PHA synthase
Metal-binding peptides
Biosorption
Contact assay

ABSTRACT

Cadmium (Cd)-contaminated waterbodies are a worldwide concern for the environment, impacting human health. To address the need for efficient, sustainable and cost-effective remediation measures, we developed innovative Cd bioremediation agents by engineering *Escherichia coli* to assemble poly(3-hydroxybutyric acid) (PHB) beads densely coated with Cd-binding peptides. This was accomplished by translational fusion of Cd-binding peptides to the N- or C-terminus of a PHB synthase that catalyzes PHB synthesis and mediates assembly of Cd2 or Cd1 coated PHB beads, respectively. Cd1 beads showed greater Cd adsorption with 441 nmol Cd mg^{-1} bead mass when compared to Cd2 beads (334 nmol Cd mg^{-1} bead-mass) and plain beads (238 nmol Cd mg^{-1} bead-mass). The Cd beads were not ecotoxic and did attenuate Cd-spiked solutions toxicity. Overall, the bioengineered beads provide a means to remediate Cd-contaminated sites, can be cost-effectively produced at large scale, and offer a biodegradable and safe alternative to synthetic ecotoxic treatments.

1. Introduction

The worldwide economic needs incessantly boost industrial, agricultural and mining activities (Tilman et al., 2011), resulting in the rising of metal contamination (Mueller et al., 2012). Cadmium (Cd) is one of the most generated metals (Martinis et al., 2009; Williams et al., 2009), of which the distribution, persistence, and toxicity severely jeopardize aquatic systems and water-supply quality (Schaider et al., 2014), adversely impacting wildlife (Alho et al., 2019) and human health (Carvalho, 2017). Water quality regulations have prioritized Cd as a hazardous substance (European Comission, 2008) and urgently call for sustainable strategies towards its removal from contaminated (waste)waters.

Bioremediation is an attractive approach for metal removal and/or stabilization (Liu et al., 2019) as it is effective for low metal-concentrations, economical, and sustainable (Li and Tao, 2015). Living organisms have been evaluated for Cd biosorption, including cyanobacteria (Zhou et al., 2014), fungi (Huang et al., 2015) and algae (Suresh Kumar et al., 2015). To improve Cd selectivity and removal capacity, genetically modified organisms (GMOs) have been produced to display, for example, histidine-rich peptides (Xu and Lee, 1999), phytochelatins (Bae et al., 2000), and metallothioneins (Blindauer, 2011; Sousa et al., 1998). However, living organisms used as a direct Cd-removal means pose limitations due to their: (1) tolerance to metal toxicity; (2) growth requirements and plasticity to cope with environmental fluctuations; (3) limited biomass production; (4) modulation of natural microbial assemblages through biostimulation/bioaugmentation

Abbreviations: Cd, cadmium; Cd1, beads displaying cd-binding peptides (Cd1) fused to the C-terminus of PhaC synthase; Cd2, beads displaying Cd-binding peptides (Cd2) fused to the N-terminus of PhaC synthase; DHA, dehydrogenase activity; DLS, dynamic light scattering; FTIR, fourier transform-infrared; GMOs, genetically modified organisms; LC-MS, liquid chromatography mass spectrometry; NFB, non-functionalized PHB beads; PHA, polyhydroxyalkanoate; PHB, poly(3-hydroxybutyric acid); pI, isoelectric point; q, biosorption capacity; R, removal percentage; SDS-PAGE, sodium dodecyl sulfate–polyacrylamide gel electrophoresis; SEM, scanning electron microscopy; TEM, transmission electron microscopy.

* Corresponding author.
E-mail address: crmarques@ua.pt (C.R. Marques).

https://doi.org/10.1016/j.watres.2020.116357

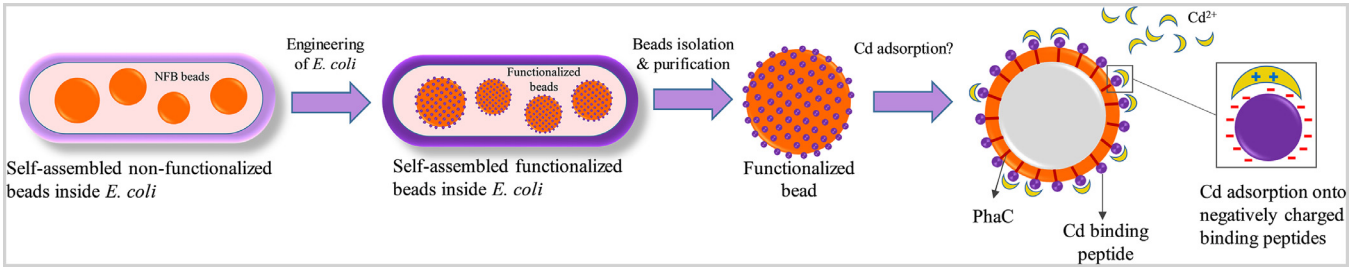

Fig. 1. Overview of synthesis and functionalization of poly(3-hydroxybutyric acid) (PHB) beads in engineered *Escherichia coli* for cadmium (Cd) adsorption. Schematic representation of PHB beads bioengineered with Cd binding peptides self-assembled inside *E. coli*, suggesting amenability toward large scale industrial application, and adsorption of Cd onto the bead surfaces occurring during bead exposure to the solutions spiked with Cd.

techniques (Marques, 2016); and (5) non-permitted release of GMOs (Liu et al., 2019; Urgun-Demirtas et al., 2006).

Alternative approaches for Cd removal have been relying on natural biosorbents originated from plants, wastes (Li et al., 2010; Mudhoo et al., 2012; Nguyen et al., 2013; Vinod et al., 2009), and microbially-synthesized exopolymeric substances (Zamil et al., 2008). Cd adsorption onto these biosorbents is dependent on the negatively-charged surfaces at specific pH (Khairy et al., 2014), which could be engineered to improve Cd-adsorption capacity. However, the chemical functionalization would result in a complex synthesis process due to the additional quality-control steps, hence, escalating the production timeline and cost. Therefore, a novel strategy that enables cost-effective biosorbent production with enhanced Cd-binding capacity is on-demand, especially when both performance and manufacturing processes, namely speed and cost, are the competitive drivers (Burakov et al., 2018).

Bacteria are naturally capable of forming spherical polyhydroxyalkanoate (PHA) beads as carbon storage inclusions (Rehm, 2010). Biodegradable poly(3-hydroxybutyric acid) (PHB) is the most commonly produced short-chain-length PHA (Parlane et al., 2017). PHB inclusions are characterized by a hydrophobic PHB core surrounded mostly by PHA synthase (PhaC) that mediates self-assembly of PHB beads (Rehm, 2010) (Fig. 1). Due to its covalent attachment to the PHB core, PhaC has been genetically engineered to anchor, immobilize and display various functional peptides/proteins at the PHB beads' surface, enabling biomedical and industrial applications (Hooks et al., 2014; Parlane et al., 2017; Rehm, 2010). Towards environmental applications, PHB beads have been functionalized with either a chromate reductase for chromium remediation (Robins et al., 2013) or an organophosphate hydrolase for organophosphorous pesticide degradation (Blatchford et al., 2012; Ogura and Rehm, 2019). Generation of large peptide libraries linked with display technologies, such as phage or whole-cell display, enabled the identification of peptides with unique metal-binding properties (Jahns and Rehm, 2012; Mejàre et al., 1998), hence allowing the informed design of PHB beads coated with respective peptides for metal sequestration, including Cd. To the best of our knowledge, the use of microbially produced PHB beads that are functionalized with Cd-binding peptides for Cd removal has not been reported yet. This approach would facilitate simultaneous synthesis and functionalization of PHB beads in one step in recombinant bacteria, avoiding multiple production steps and thus removing limitations inherent to the traditional approaches. Moreover, the use of bacteria means that the biomanufacturing processes occur at environmentally friendly conditions and that the numbers of the functionalized PHB beads can be easily multiplied by controlling the bacterial growth, hence facilitating scalable and sustainable bead production. Moreover, the covalent links between the fusion peptides and the PHB core would avoid leaching of the peptides from the beads during harsh adsorption conditions.

In this study, we designed and produced PHB beads displaying Cd-binding peptides in engineered *E. coli* (Fig. 1), and compared their production yields and performances. *E. coli* was selected as microbial cell factories for the production of PHB beads displaying Cd-binding peptides due to its well-documented genetic configuration, hence, promoting relatively easy genetic engineering (Moradali and Rehm, 2020; Rehm, 2010), as well as its ability to achieve high volumetric productivity through high cell density fermentation technology and scalable bioprocess unit operations, which have long been established for commercial biopharmaceuticals (Yee and Blanch, 1992). The Cd-biosorption abilities of the beads were analyzed under different pH and initial Cd concentrations. The environmental safety of the produced beads was primarily assessed against a bioindicator bacterium. Overall, we have demonstrated a cost-effective method to produce functionalized and biodegradable beads in one step in *E. coli*, and that the beads function as an effective and harmless alternative for Cd bioremediation.

2. Material and methods

2.1. Plasmids, strains and cultivation

Plasmids and oligonucleotides, as well as *E. coli* strains used for general cloning and plasmid propagation (XL1-Blue) and for PHA bead synthesis (BL21(DE3)) are presented in Table 1. Both bacterial strains were grown at 37 °C and 200 rpm in Luria-Bertani (LB) medium supplemented with antibiotics as appropriate.

2.2. Plasmid construction

Two nucleotides *cd*1 and *cd*2 (IDT, Germany) were designed and used to encode the Cd binding peptides HSQKVF- VDGLSCT-NCAAKFERNVKEIEGVTEAI (identified from PROSITE database by (Eskandari et al., 2013)) and $(HSQKVF)_2$-$(CTYSRLHLC)_1$ (derived from biopanning of phage display libraries (Flynn et al., 2003; Mejàre et al., 1998)), respectively. The new plasmids were constructed through in-frame insertion of *cd*1 or *cd*2 at the 3′- or 5′-end of *pha*C harbored by the plasmid pPOLY-C-PhaC, respectively. Cloning procedures as described in Hay et al. (Hay et al., 2017) and Hooks et al. (Hooks et al., 2014) were employed for generating the hybrid plasmids pPOLY-C-PhaC-linker-Cd1 and pPOLY-C-Cd2-PhaC. The plasmids sequences were confirmed by DNA sequencing (Massey Genome Service, Palmerston North, New Zealand) using T7 primers (Table 1).

2.3. Beads production, isolation and purification

Competent *E. coli* BL21(DE3) cells harboring plasmid pMCS69 were separately transformed with the newly constructed plasmids (pPOLY-C-PhaC-Linker-Cd1 and pPOLY-C-Cd2-PhaC) and the

Table 1
E. coli strains, plasmids and oligonucleotides used in the present study.

Bacterial strains	**Genotype**	**Source**
E. coli XL1-Blue	*recA1 endA1 gyrA96 thi-1 hsdR17 supE44 relA1 lac [F′ proAB lacI^q ZΔM15 Tn10 (Tet^r)]*	Stratagene
E. coli BL21(DE3)	*F-, ompT, hsdS (rB$^-$ mB$^-$), gal λ, dcm (DE3)*	Novagen
Plasmids	**Description**	**References**
pMCS69	Cm^r; pBBR1MCS derivative containing genes *phaA* and *phaB* from *Ralstonia eutropha*	Amara and Rehm (Amara and Rehm, 2003)
pPOLY-C-PhaC	Amp^r; pET-14b derivative containing *phaC* from *R. eutropha*, and *StuI, XhoI, XmaI* and *Bam*HI sites downstream of *phaC*	Hay et al. (Hay et al., 2017)
pPOLY-C-PhaC-linker-Cd1	pPOLY-C-PhaC derivative containing Cd-binding motif inserted at the *phaC* C terminus into *Bam*HI/*XhoI* sites. The Linker in between proteins promotes their folding and independent functionality (Jahns and Rehm 2009)	This study
pPOLY-C-Cd2-PhaC	pPOLY-C-PhaC derivative containing Cd-binding motif inserted at *phaC* N terminus into *XbaI/SpeI* sites.	This study
Oligonucleotides	**Sequence 5′ - 3′**	**References**
C-phaC_fwd	AGC CAC TGG ACT AAC GAT GC	This study
N-phaC_rev	TCG AAT GGC CCC GGC GTG ACC TTG AAT G	This study

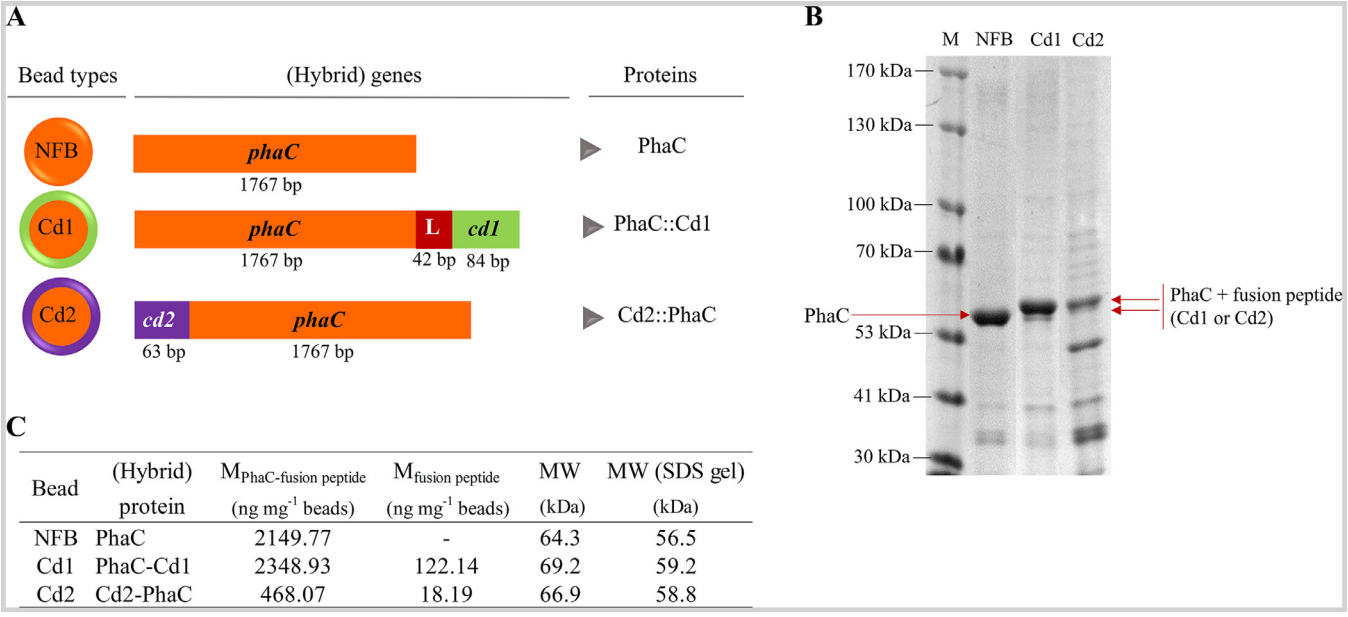

C

Bead	(Hybrid) protein	$M_{PhaC\text{-}fusion\ peptide}$ (ng mg^{-1} beads)	$M_{fusion\ peptide}$ (ng mg^{-1} beads)	MW (kDa)	MW (SDS gel) (kDa)
NFB	PhaC	2149.77	-	64.3	56.5
Cd1	PhaC-Cd1	2348.93	122.14	69.2	59.2
Cd2	Cd2-PhaC	468.07	18.19	66.9	58.8

Fig. 2. Design and production of poly(3-hydroxybutyric acid) (PHB) beads displaying cadmium binding peptides. (**A**) Bead types produced and the respective hybrid genes (direction: 5′ to 3′) and proteins (bp – base pairs; NFB – non-functionalized bead; Cd1 – PhaC-linker-Cd1-displaying beads; L – linker; Cd2 – Cd2-PhaC-displaying beads; *phaC* – gene encoding PhaC; *cd1* – gene encoding the Cd-binding peptide Cd1; *cd2* – gene encoding the Cd-binding peptide Cd2). (**B**) Sodium dodecyl sulfate–polyacrylamide gel electrophoresis (SDS-PAGE) analyses of the fusion proteins displayed on NFB, Cd1 and Cd2 beads. Lane 1 – protein molecular weight (kDa) marker (GangNam-Stain™, iNtRON Biotechnology, Seongnam, South Korea); lane 2 – NFB beads showing PhaC protein (56.5 kDa); lane 3 – Cd1 beads displaying PhaC-linker-Cd1 (59.2 kDa); lane 4 – Cd2 beads surface-displaying Cd2-PhaC (58.8 kDa). (**C**) Amount (mass, M) of PhaC protein and PhaC-fusion protein hybrid (*i.e.*., Cd1 or Cd2) expressed per mass of beads, the respective theoretical and protein-marker-based molecular weights (MW), and theoretical isoeletric point (pI; computed in ExPASy Bioinformatics Portal).

wildtype pPOLY-C-PhaC (Fig. 2A). The plasmid pMCS69 enables the production of the precursor *R*-3-hydroxybutyrate-coenzyme A, which mediates the production of PHA beads (Rubio Reyes et al., 2016). *E. coli* BL21(DE3) transformants were cultured at 37°C in LB medium containing ampicillin, chloramphenicol and 1% (w/v) D-glucose. At an OD_{600} (optical density at 600 nm) of 0.6–0.8, the PHA bead production was induced by addition of 1 mM isopropyl-β-D-thiogalactopyranoside into the cultures, which were further incubated for 48 h at 25°C (Hay et al., 2017).

The cells were harvested, washed and subjected to mechanical cell disruption (CF1 cell disrupter, Constant Systems Ltd, UK) in a lysis buffer, followed by purification and storage of the purified beads as described elsewhere (Hay et al., 2017; Rubio Reyes et al., 2016).

2.4. Beads characterization

Fusion proteins on the beads were separated in a sodium dodecyl sulfate–polyacrylamide gel electrophoresis (SDS-PAGE) (Rubio Reyes et al., 2016). The amount of Cd-binding peptides displayed on the surface of each bead type was determined through densitometric analysis based on the standard curve computed from a range of bovine serum albumin concentrations. Gel images were analyzed with Image Lab Software (Version 3.0 build 11, Bio-Rad Laboratories, USA), and the amount of Cd-binding peptide was expressed as ng peptide per mg of beads (Hay et al., 2017; Rubio Reyes et al., 2016). The fusion protein sequences were confirmed by liquid chromatography - mass spectrometry (LC-MS) after trypsin (for all fusion proteins), chemotrypsin or endopro-

teinase AspN (for Cd2-PhaC fusion protein) digestions of the excised SDS-PAGE gel-bands.

The morphology of the beads was observed under transmission electron microscopy (TEM) and scanning electron microscopy (SEM). The preparation of samples for TEM followed procedures previously explained (González-Miró et al., 2018). Prior to SEM analyses, the beads were sputter-coated with an ultrathin layer of platinum in an argon atmosphere to make them electronically conductive.

The PHB content of beads was analyzed by Fourier transform-infrared spectroscopy (FTIR; Perkin Elmer FTIR Spectrometer equipped with a horizontal cell Golden Gate™). Spectra data were collected in the transmission mode by averaging 64 scans over wavenumber ranges of 4000–500 cm^{-1} at a spectral resolution of 4 cm^{-1}. A commercial PHB (Sigma-Aldrich, Germany) was used as a standard for comparison means.

The zeta potentials (ζ), Z-average diameters (d) and dispersity (Đ) of the purified beads were determined by dynamic light scattering (DLS), using Zetasizer Nano-ZS (Malvern Panalytical, Malvern, U.K.). The beads were diluted prior to size measurement to avoid multiple scattering effects. Zeta potential was measured in a 0.1% (w/v; wet weight) dispersion in either ultrapure water or a 10 mM NaCl solution at different pH (3, 5, 7, 9). All measurements were performed in triplicate.

2.5. Cd binding assays

Each of the three bead variants (NFB, Cd1 and Cd2) at the density of 1% (w/v; wet weight) was incubated in 1.5 mL of either ultrapure water or Cd solution (as $CdCl_2{\cdot}2{\cdot}5H_2O$, CAS: 7790–78–5, Sigma-Aldrich; in ultrapure water) at 20±0.5°C and 180 rpm in an orbital shaker for 60 mins (*i.e.,* the equilibrium time according to our preliminary trials). Cd adsorption by beads was conducted at different initial concentrations of Cd (0, 0.01, 0.1, 1, 3 mM) which were set according to its toxicity and concentrations detected in low- and highly-contaminated effluents or waterbodies (Neiva et al., 2014). Considering that metal speciation is affected by the pH of such aquatic systems, the Cd adsorption was evaluated at pH 3, 5, 7 and 9. The assays were conducted in triplicates per treatment for each bead type, and after the exposure to metal solutions the beads were recovered by centrifugation.

Cd concentrations in the initial solutions (*i.e.,* before contact with the beads) and in the aqueous supernatant (*i.e.,* after contact with the beads) were quantified by inductively coupled plasma atomic emission spectroscopy (ICP-AES) (Horiba Jobin Yvon ULTIMA, Edison, NJ). Cd-adsorption capacity (q, nmol Cd mg^{-1}) and removal percentage (R,%) of the beads were calculated by equations (1) and (2):

$$(1)\ q = [(C_i - C_f) / m_b] / V$$
$$(2)\ R = [(C_i - C_f) / C_i] \times 100,$$

where C_i represents the Cd initial concentration in solution (nmol L^{-1}), C_f is the Cd concentration in solution after contact with the beads (nmol L^{-1}), m_b (mg) is the bead mass (dry weight, dw), and V is the volume of the test solution (0.0015 L). q_e and C_{eq} represent the adsorption capacity and Cd concentration at equilibrium, respectively (Martins et al., 2017).

Langmuir, Freundlich, and Sips adsorption isotherms were applied to fit the experimental equilibrium data (average of three replicates) of the Cd binding assays performed at pH 7 and 9. Langmuir model assumes a homogeneous distribution of binding sites and monolayer adsorption on the adsorbent surface, while the empirical Freundlich isotherm describes multilayer adsorption onto highly heterogeneous surfaces (Martins et al., 2017). Sips, in turn, is a combination of both models (Zahri et al., 2017). Non-linear regression curves were derived for each bead variant through the least-squares method based on the equations (3, 4, 5) below:

$$(3)\ \text{Langmuir}\ q_e = (Q_{max} * K_L{*}C_{eq}) / (1 + K_L{*}C_{eq})$$
$$(4)\ \text{Freundlich}\ q_e = K_F * C_{eq}{}^{N}$$
$$(5)\ \text{Sips}\ q_e = [Q_{max} * (K_S{*}C_{eq})^{Y}] / [1+(K_S{*}C_{eq})^{Y}]$$

where q_e (nmol Cd mg^{-1}) is the bead adsorption capacity at equilibrium, Q_{max} (nmol Cd mg^{-1}) is the maximum adsorption capacity, C_{eq} (nmol L^{-1}) is the Cd concentration at equilibrium, K_L (L mg^{-1}), K_F (nmol$^{1\text{-}N}$ L^N mg^{-1}) and K_S (L mg^{-1}) are the adsorption constants related with the adsorption capacity (q_e) of the adsorbent at equilibrium, and N (=1/n) is a unitless parameter usually associated with the adsorption intensity in Freundlich model.

2.6. Ecotoxicity assays

The toxicity of Cd-bound and Cd-unbound beads (NFB, Cd1 and Cd2) from the metal-binding assays was evaluated against the bacterium *A. globiformis* (decomposers). The toxicity of metal solutions before and after the Cd binding assays was assessed against *A. globiformis*. Although the *A. globiformis* contact tests are usually applied to evaluate the effect of solid samples (*e.g.,* wastes) in the bacteria DHA (ISO, 2016), it has been successfully used in our lab for testing aqueous samples (unpublished data). Briefly, the Cd-bound and Cd-unbound beads were resuspended in 600 µL of distilled water to achieve a bead density of 1% (w/v). For the aqueous phase tests, 600 µL of the supernatants obtained after centrifugation of the remediated solutions at the end of metal-binding assays was considered. At least three replicates were performed per treatment. An exponentially growing *A. globiformis* inoculum (OD_{600} = 0.4) was added to each test well (400 µL). The kinetics of the DHA-assisted conversion of resazurin into the fluorescent resorufin compound was fluorimetrically followed for 1 h after adding 800 µL of the resazurin buffer. *A. globiformis* response was computed as the average percentage (%) inhibition of DHA (Marques et al., 2018, 2014).

2.7. Statistics

A one-way analysis of variance (one-way ANOVA) followed by the Tukey multiple comparison test were performed to test significant differences of zeta potentials of all the beads for each pH tested. A two-way ANOVA was carried out to evaluate the influence of the two factors (*i.e.,* Cd concentration and bead type (or no bead)) and their interactions on the adsorption and removal capacities of beads as well as on the response of *A. globiformis* under different pH. If no significant interaction was determined, the influence of each factor was tested within each level of the other factor by the one-way ANOVA followed by the Tukey test. If a significant interaction was detected, a similar approach was conducted, except that the $MS_{residual}$ of the two-way ANOVA was considered for the calculation of the one-way ANOVA F and the q statistics for the Tukey test (Quinn and Keough, 2002). Statistics were performed using SigmaPlot 11.0, and a significant result was considered whenever $P \leq 0.05$.

3. Results

3.1. Design and production of Cd-binding peptide-coated PHB beads

Hybrid genes were constructed as to encode two different Cd-binding peptides, Cd1 or Cd2, fused to either C- or N-terminus of PhaC synthase, respectively. The Cd-binding peptide motifs had been selected based on their affinity, selectivity and improved capacity to bind Cd using phage display (Flynn et al., 2003) or bacterial cell surface display systems (Eskandari et al., 2013;

Mejàre et al., 1998). The orientation and constraint of the peptides during biopanning studies informed on how to translational fuse the peptides to the PHB synthase (*i.e.,* the PHB anchoring domain). In addition, PhaC engineering aimed to facilitate high production yields of PHB beads densely coated with peptides that retained structural flexibility to interact with Cd in bulk solutions (Fig. 1). A linker was used when fusing Cd1 to the C-terminus of PhaC to retain hydrophobic PHB core formation combined with the enhanced display of Cd1 peptides on the PHB bead surface (Jahns and Rehm, 2009). Therefore, two plasmids, pPOLY-C-PhaC-linker-Cd1 or pPOLY-C-Cd2-PhaC, were constructed by inserting either *cd*1 or *cd*2 genes encoding for Cd1 or Cd2 peptides into the 3′- or 5′-end of *pha*C, respectively, based on original screening of the peptides and their validation (Fig. 2A). *E. coli* BL21(DE3) harboring plasmid pMCS69, which encodes for PhaA and PhaB proteins that sequentially catalyze the synthesis of PHB precursors (Rubio Reyes et al., 2016), was transformed with each of the plasmids to mediate the synthesis of Cd1-peptide-coated (Cd1) and Cd2-peptide-coated (Cd2) PHB beads, respectively. As a control, *E. coli* BL21(DE3) harboring pMCS69 was also transformed with the plasmid pPOLY-C-PhaC to produce nonfunctionalized PHB beads (NFB) (Fig. 2A). The biomanufacturing processes revealed that production yields for NFB, Cd1 and Cd2 beads were 7.1, 8.1 and 2.0%, respectively.

3.2. Characterization of the beads

SDS-PAGE analyses on the protein profiles of isolated NFB, Cd1 and Cd2 beads indicated successful production of the respective proteins. SDS-PAGE of the purified NFB qualitatively showed the dominant band at 56.5 kDa (Fig. 2B), which corresponds to the molecular weight of PhaC. The fusion proteins PhaC-linker-Cd1 or Cd2-PhaC attached to Cd1 or Cd2 beads were also produced as indicated by the protein bands having higher molecular weight, *i.e.,* 59.2 or 58.8 kDa (Figure 2B), respectively, than only PhaC. The amount of Cd-binding peptides coating the beads was quantified to be 122.14 ng mg^{-1} Cd1 beads and 18.19 ng mg^{-1} Cd2 beads based on densitometry analyses (Fig. 2C). LC-MS tryptic peptide fingerprinting of proteins excised from SDS-PAGE gels confirmed the expected protein sequence of PhaC, PhaC-linker-Cd1 and Cd2-PhaC (Table S1).

TEM images showed that all the beads were formed inside the recombinant *E. coli* (Fig. 3, upper panel), indicating that the PhaC synthase in the fusion proteins remained fully functional mediating *in vivo* PHB bead formation. Further TEM (Fig. 3, middle panel) and scanning electron microscopy (SEM) (Fig. 3, bottom panel) images showed the intact and mostly spherical morphology of the purified beads. The hydrodynamic diameters of NFB, Cd1 and Cd2 beads as determined by DLS were 1708±101, 1299±26, and 1146±74 nm (Fig. 3), respectively, with a dispersity (Đ) <0.2.

Such variation on the size of different functionalized beads was previously observed (González-Miró et al., 2018; Rubio Reyes et al., 2016), but the associated causes remain unclear.

The FTIR spectra of the three beads were compared with that of the commercial PHB standard, evidencing nearly identical spectra (Figure S1), thereby confirming that the beads were composed of PHB. The characteristic spectra of beads' PHB can be identified by the peaks at 1720, between 1050 and 1230, 1270, and 1452 cm^{-1}, which are assigned to *C=O* and C–O stretching of the ester group and C–H asymmetrical deformations of the CH_2 and CH_3 groups, respectively. Additionally, the doublet between 2860 and 3000 cm^{-1} can be attributed to the stretching of C–H bond. The bands of minor relevance at around 2300–2400 cm^{-1} found in all spectra are likely associated with CO_2 in the atmosphere. In general, FTIR spectra profiles of our beads are in good agreement with those of PHB inclusions synthesized by *Cupriavidus necator* (Oliveira et al., 2007).

Considering that Cd adsorption can occur through electrostatic attraction (Mudhoo et al., 2012), we determined zeta potentials of the beads dispersed in either water or saline solution at different pH as a proxy to understand the magnitude of electrostatic interactions between metal-binding active sites on the bead surfaces and Cd in the bulk solution. Zeta potentials of the beads in saline solution were lower than those in water, as the salts reduce the absolute zeta potentials (Fig. 4). The beads were positively charged at pH 3, but when increasing the pH to about 5, beads' zeta potentials decreased to their isoelectric points (pI). Accordingly, the pI of NFB, Cd1 and Cd2 beads dispersed in water were estimated to be 4.88, 5.03 and 4.70 (Fig. 4A), whereas in saline solution it shifted to 5.23, 6.96 and 5.49, respectively (Fig. 4B). Further increase in pH resulted in negative zeta potentials of the beads, particularly at pH 9. The absolute zeta potential values obtained for NFB dispersed in saline solutions were in agreement with the values previously reported for PHB beads that were designed for vaccine purposes (González-Miró et al., 2018).

3.3. Use of engineered PHB beads for Cd bioremediation

All PHB beads were subjected to metal-binding assays to assess Cd biosorption capacity (q) and removal% (R) at various pHs and initial Cd concentrations (Fig. 5). At pH 5, q and R were either negative or zero (data not shown), suggesting that no beads sequestered Cd at the pH close to the beads' pI (Figs. 2C and 5). Nevertheless, when the pH was set to 3, 7 and 9, both q and R were progressively increased, indicating that the beads were able to sequester Cd at pH values distant from beads' pI. The%Cd removal (R) by Cd1 and Cd2 beads was in the range of 10–41% and 47–89% at pH 7 and 9, respectively, reaching their highest R values at pH 9 (Fig. 5, Tables S2-S3), at which beads were negatively charged (Fig. 4). Maximum Cd adsorption at pH 9 had also been observed by others (Copello et al., 2008; Li et al., 2010; Zahri et al., 2017). Since Cd could precipitate at pH≥9 as $Cd(OH)_2$ and mislead the interpretation of biosorption mechanisms (Copello et al., 2008), the initial Cd concentration of 3 mM in a solution exposed to beads was corrected by subtracting the average amount of precipitated Cd in a 3 mM Cd solution not exposed to the beads.

In general, increasing initial Cd concentrations from 0.01 to 1 mM enhanced beads q (Fig. 5, Tables S2-S3). However, when the initial Cd concentration was increased from 1 to 3 mM at pH 7, both q and R of Cd2 beads decreased. Under the same initial Cd concentrations at pH 9, the q of Cd1 beads was only slightly increased, while R was decreased. The decreasing trends of q and R extent at high Cd concentrations suggested exhaustion of the available Cd-binding sites at Cd1 and Cd2 beads surface (Martins et al., 2017). Overall, both Cd1 and Cd2 beads demonstrated significantly higher q and R for Cd biosorption than NFBs, providing evidence for successful display and functionality of the Cd-binding peptides Cd1 and Cd2, respectively. In particular, the Cd2 peptide showed strong Cd adsorption of 2.8–20.8 nmol Cd ng^{-1} peptide compared to the Cd1 peptide (0.2–3.8 nmol Cd ng^{-1} peptide) under adsorption-promoting conditions (*i.e.,* at pH 9 for initial Cd concentrations ranging from 0.01 to 3 mM). Notwithstanding, the amount of Cd1 peptide coating Cd1 beads is higher (122.14 ng mg^{-1} bead mass) compared to that of Cd2 beads (18.19 ng mg^{-1} bead mass) (Fig. 2C), which ultimately had enhanced the adsorption capacity and Cd removal% of Cd1 beads.

Equilibrium studies were conducted in order to assess the underlying adsorption mechanism(s) at pH 7 and 9, where q and R showed the highest levels (Fig. 5). Fig. 6 depicts the non-linear regression curves resulting from the fitting of three adsorption isotherms to the experimental data. Sips was the model better describing Cd removal at both pHs by all the beads (NFB, Cd1, and Cd2), achieving the highest correlation values (R^2>0.990),

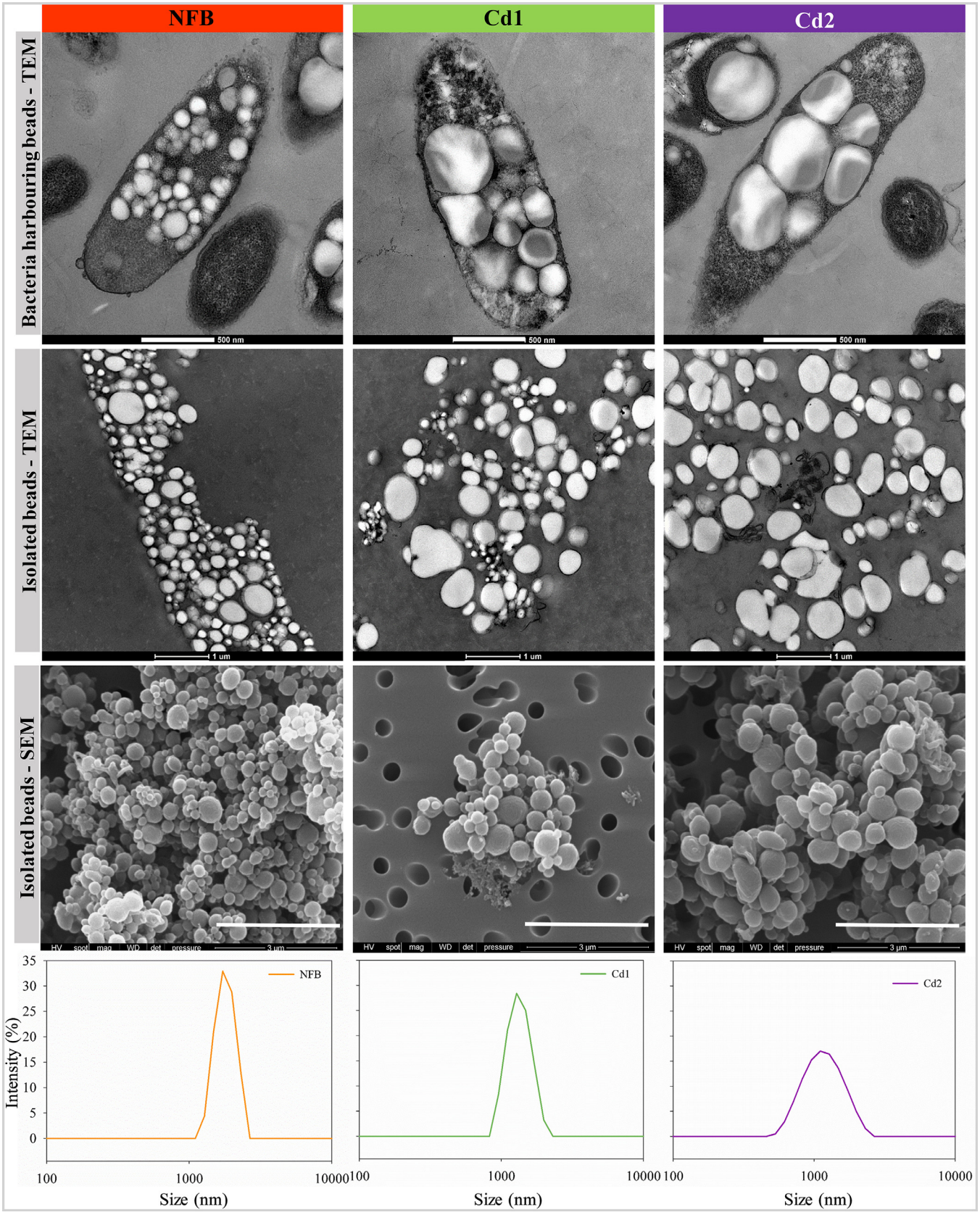

Fig. 3. Characterization of *Escherichia coli* inclusions of PHB beads and the isolated PHB beads. Top panel: TEM images of *E. coli* BL21(DE3) containing self-assembled beads (*NFB* – non-functionalized beads; *Cd1* – PhaC-linker-Cd1-displaying beads; *Cd2* – Cd2-PhaC-displaying beads) (scale bar: 500 nm). Second from the top panel: TEM images of the respective isolated and purified beads (scale bar: 1 µm). Third from the top panel: SEM images of the purified beads (scale bar: 3 µm). Bottom panel: size distribution of the three beads as measured based on the dynamic light scattering. Note: *cd1*/Cd1 and *cd2*/Cd2 are used with nomenclatural purposes only, and do not represent the name of deposited genes or proteins in available databases.

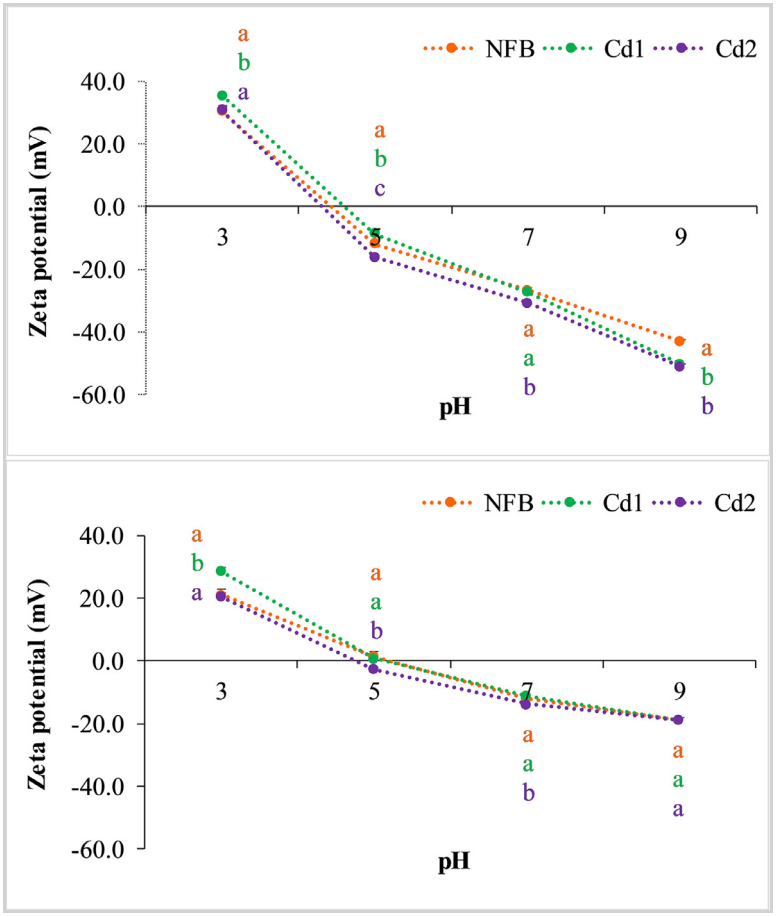

Fig. 4. Variation of the zeta potentials of the three bead types (NFB – non-functionalized beads; Cd1 and Cd2 – the two functionalized beads for Cd binding). Zeta potentials of the beads were determined upon their dispersal in water (**A**) and in a 10 mM NaCl solution (**B**) at different pH. Error bars represent standard deviation. Different letters highlight statistically significant differences of zeta potentials among the beads for each pH ($P \leq 0.05$).

whereas Langmuir (R^2: 0.739–0.985) and Freundlich (R^2: 0.683–0.999) isotherms fitted only for specific beads at specific pH values. Furthermore, the maximum adsorption capacity (Q_{max}) retrieved by Sips was quite similar to the average q determined for each bead variant exposed to solutions containing 3 mM Cd, either at pH 7 (NFB: 128.1, Cd1: 268.1, Cd2: 133.4 nmol Cd mg^{-1} bead mass) or pH 9 (NFB: 262.8, Cd1: 268.1, Cd2: 458.1 nmol Cd mg^{-1} bead mass).

3.4. Are the bioengineered PHB beads harmless and effective?

We evaluated the beads suitability towards potential environmental applications regarding their safety and efficiency for Cd bioremediation. This assessment was obtained by determining the effect of non-exposed (*i.e.,* at 0 mM Cd) and Cd-exposed beads on the inhibition of dehydrogenase activity (DHA) of the bacterium *Arthrobacter globiformis* (Fig. 7, Tables S4-S5). *A. globiformis* is a ubiquitous bacterium, which synthesizes dehydrogenase – an enzyme involved in many essential mechanisms sustaining bacterial survival (*e.g.,* respiration) that is sensitive to metals (ISO, 2016; Marques et al., 2018; 2014).

All the beads that were not exposed to Cd were considered not toxic as they did not inhibit DHA. In contrast, DHA was significantly impaired by Cd1 and Cd2 beads with bound Cd, when compared to the outcome obtained for Cd-bound NFBs (Fig. 7, Tables S4-S5). This trend was particularly observed for Cd1 and Cd2 beads previously exposed to high Cd concentrations at both pH 7 (from 0.01 to 3 mM Cd) and pH 9 (at 1 and 3 mM Cd). These findings consistently emphasize the remarkable ability of Cd1 and Cd2 beads for Cd biosorption, in contrast with NFBs that bound much less Cd and hence were less hazardous.

An efficient bioremediation is achieved whenever the bioremediation agents are capable of sequestering Cd to levels that reduce the ecotoxic potential of contaminated samples/environments (Pandey et al., 2009). The inhibitory effect of Cd solutions after being remediated by the engineered beads at increasing pH was significantly decreased (Fig. 8, Table S6). For initial Cd concentrations of ≤0.1 mM (at pH 7) or ≤1 mM (at pH 9), Cd1 and Cd2 beads could effectively remove Cd, since the corresponding remediated solutions were nontoxic for *A. globiformis*, considering that 30% DHA inhibition is the threshold value below which no toxicity is detectable. At higher initial Cd concentrations, both at pH 7 and 9, the beads-remediated solutions remained toxic to *A. globiformis* with over 30% of DHA inhibition. Although NFB could apparently retain certain amounts of Cd (under pH 7 and 9), and consequently lower the toxicity of remediated Cd solutions, this was negligible as compared to the bioremediation efficiency of Cd1 and Cd2 beads (Fig. 8).

4. Discussion

The selection and expression of metal-binding peptides are crucial steps in generating metal bioremediation agents. These peptides should not only exhibit metal affinity but, when bioengineering PHB beads, should also be amendable toward translational fusion to the PHB synthase to enable overproduction of *in vivo* self-assembled PHB beads displaying the metal-binding peptides (Hooks et al., 2014; Parlane et al., 2017). Besides high-yield produc-

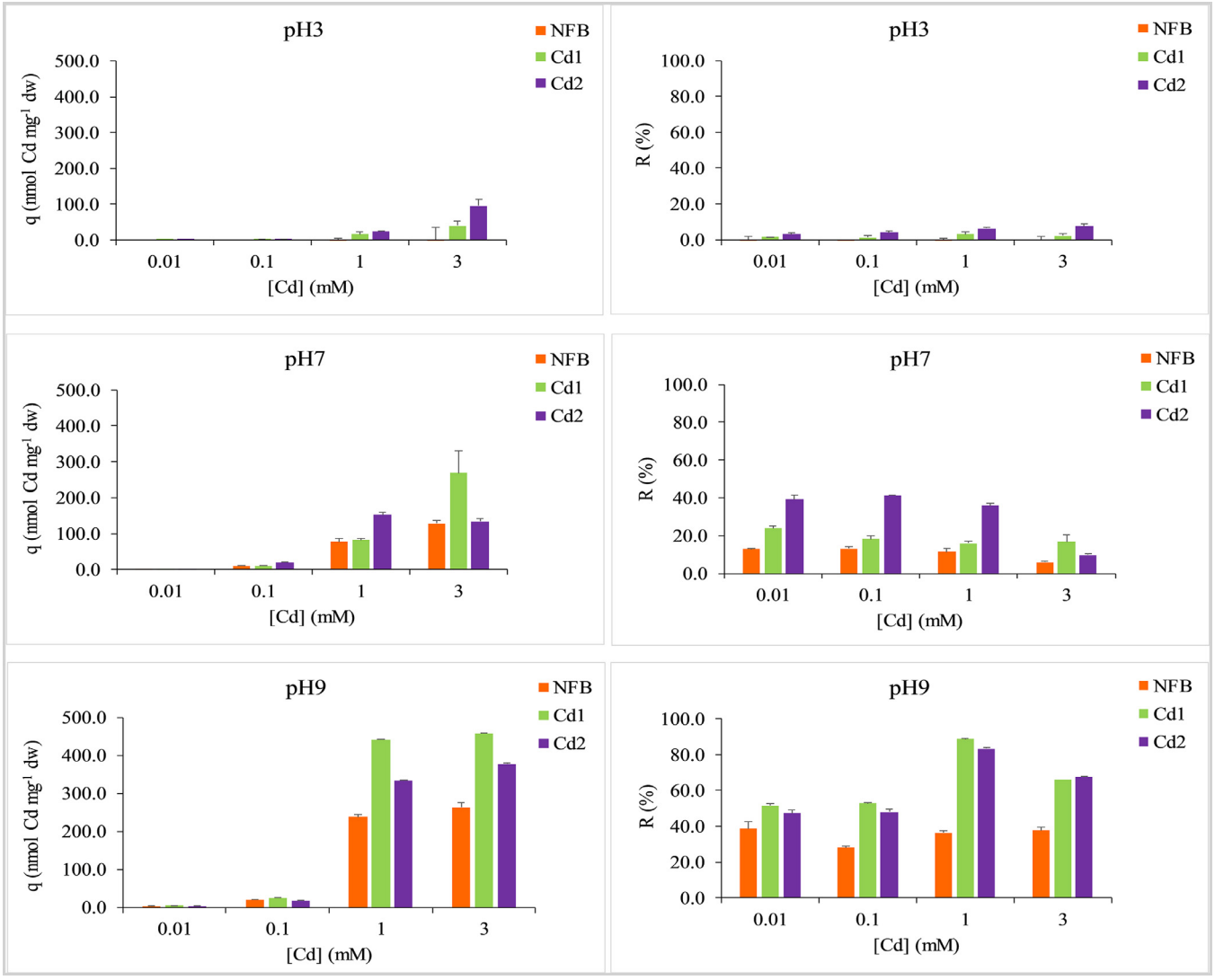

Fig. 5. Adsorption (q) and removal (R) capacity of Cd by the NFB, Cd1 and Cd2 beads. The parameters were computed for NFB, Cd1 and Cd2 beads at the density of 1% (w/v; wet weight) under different initial Cd concentrations and pH. Error bars represent standard deviation. The outcome of the statistical analyses performed to the data is provided in Tables S2 and S3.

tion, protein engineering strategies also need to address the retention of metal-peptide interactions for enhanced metal adsorption capacity (Eskandari et al., 2013).

Here we bioengineered *E. coli* as cell factories to assemble and produce novel PHB beads densely coated with Cd-binding peptides. This was achieved by selecting Cd-binding peptides and protein-engineering approaches that retained functionality of PHB-bead-forming enzyme (PhaC), while enabling overproduction of the peptides aligned with functional orientation for efficient Cd binding (Figs. 1 to 5). Cd1 and Cd2 beads showed q and R functions two times more enhanced than NFBs, particularly at neutral to basic pH (Fig. 5, Tables S2-S3). Moreover, the Cd2 beads were overall capable of Cd sequestration at levels that rival those described for His-rich (poly)peptides (Sousa et al., 1998), Cys-rich peptides (Bae et al., 2000), metallothioneins (Sousa et al., 1998) or naturally occurring Cd-binding domains (Eskandari et al., 2013), engineered for cell surface display in recombinant hosts towards Cd bioremediation (Table S7).

Cd is present as a metallic cation (Cd^{2+}) in aqueous solution, and its biosorption has been broadly associated with complexation or coordination mechanisms, resulting from metal interaction with negatively charged sites on biomass or biomaterials (Mudhoo et al., 2012). Consequently, pH may influence the adsorption of Cd due to changes on the electronegativity and hence reactivity of binding sites, as well as on metal speciation in solution. PHB inclusions are characterized by a PHB core that is coated by several proteins at the shell (Rehm, 2010), of which polarity, hydrophilicity/hydrophobicity and charge depend on both amino acids composition and pH (Lide, 2005). Therefore, it was not surprising that NFB also showed a certain level of Cd-adsorption capacity and removal, especially due to their negative charges at basic pH (Fig. 5). However, the functional peptides Cd1 and Cd2 displayed on Cd1 and Cd2 beads, respectively, improved Cd adsorption capacity, by providing additional binding sites for Cd^{2+}. Among the amino acids composing Cd1- and Cd2-binding peptides, serine, cysteine, threonine, asparagine, glutamate and histidine residues have been widely associated with higher Cd affinity (Blindauer, 2011; He et al., 2012; Mejàre et al., 1998). The engineered motifs present a high percentage of negatively charged amino acids (15% in Cd1 beads; *i.e.,* aspartate and glutamate) and/or of polar amino acids (30% for Cd1 and 57% for Cd2 beads; *e.g.,* serine, threonine, cysteine, tyrosine, asparagine and glutamine). Under basic pH values (*i.e.,* above the respective amino acids pKa), these polar residues tend to present a negative net charge given by the ionization of carboxyl, amino, hydroxyl or sulfhydryl acidic functional groups (Khairy et al., 2014).

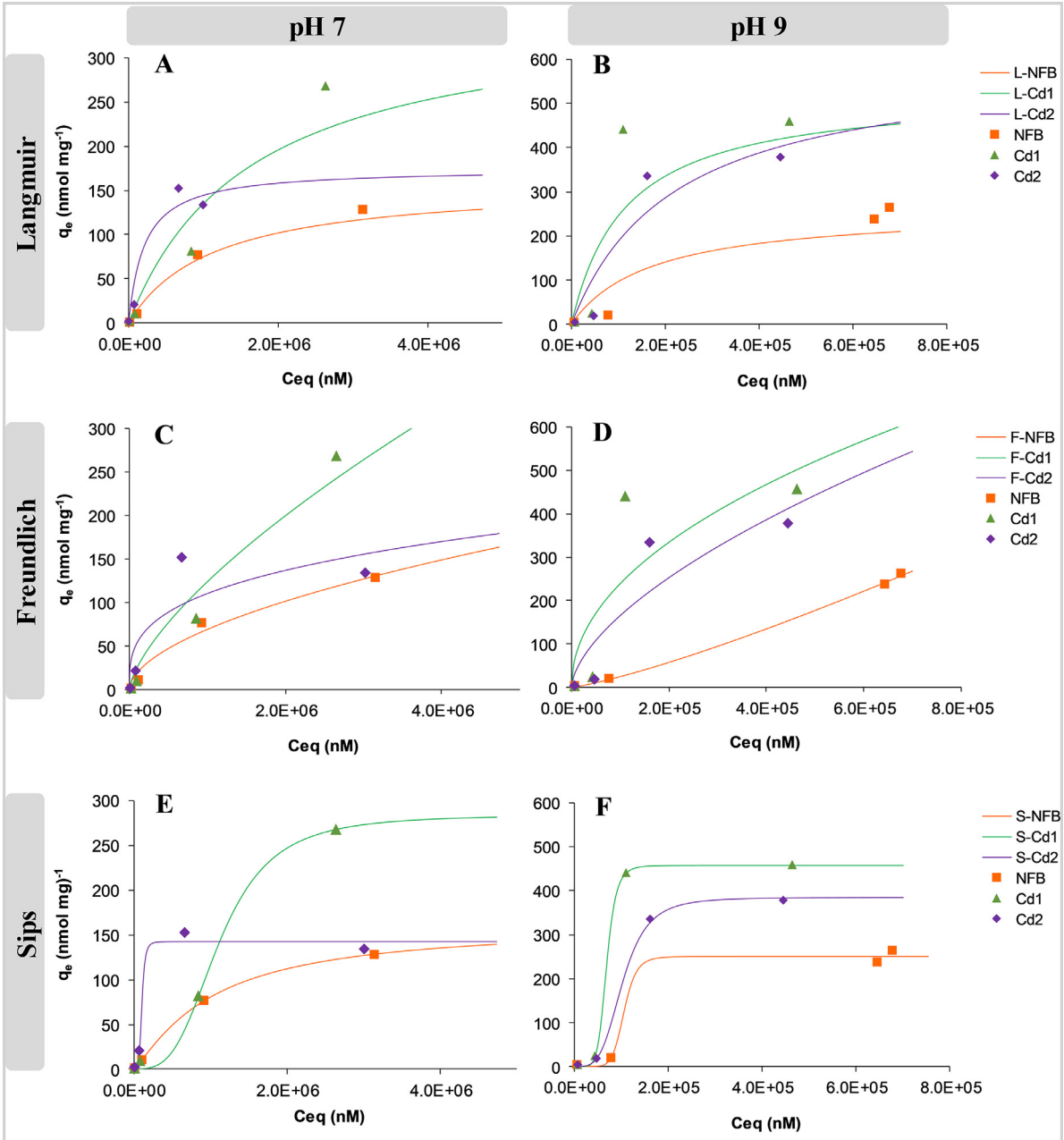

pH7

Beads	Langmuir Q_{max} (nmol mg^{-1})	Langmuir K_L (L mg^{-1})	Langmuir R^2	Freundlich K_F (nmol^{1-N} L^N mg^{-1})	Freundlich N	Freundlich R^2	Sips Q_{max} (nmol mg^{-1})	Sips K_S (L mg^{-1})	Sips ɣ	Sips R^2
NFB	159.42	8.79E-07	0.985	0.03	0.553	0.979	161.29	9.93E-07	1.189	1.000
Cd1	356.241	6.10E-07	0.914	0.01	0.688	0.963	284.31	8.95E-07	3.254	0.998
Cd2	174.30	4.75E-06	0.940	1.49	0.311	0.734	142.68	9.80E-06	5.029	0.990

pH9

Beads	Langmuir Q_{max} (nmol mg^{-1})	Langmuir K_L (L mg^{-1})	Langmuir R^2	Freundlich K_F (nmol^{1-N} L^N mg^{-1})	Freundlich N	Freundlich R^2	Sips Q_{max} (nmol mg^{-1})	Sips K_S (L mg^{-1})	Sips ɣ	Sips R^2
NFB	262.00	5.84E-06	0.865	1.74E-05	1.230	0.999	250.19	9.44E-06	8.132	0.994
Cd1	527.83	8.71E-06	0.739	0.91	0.484	0.683	456.93	1.46E-05	6.758	1.000
Cd2	602.47	4.54E-06	0.874	0.15	0.612	0.814	384.91	9.72E-06	3.885	0.999

Fig. 6. Adsorption isotherm models applied for Cd biosorption by the NFB, Cd1 and Cd2 beads. Langmuir (A, B), Freundlich (C, D), and Sips (E, F) models were fitted to the experimental data obtained for the three bead types at pH 7 and 9, and 20°C. Model parameters are provided in the tables below the plots. q_e and C_{eq} represent adsorption capacity at equilibrium and cadmium concentration in solution at equilibrium, respectively.

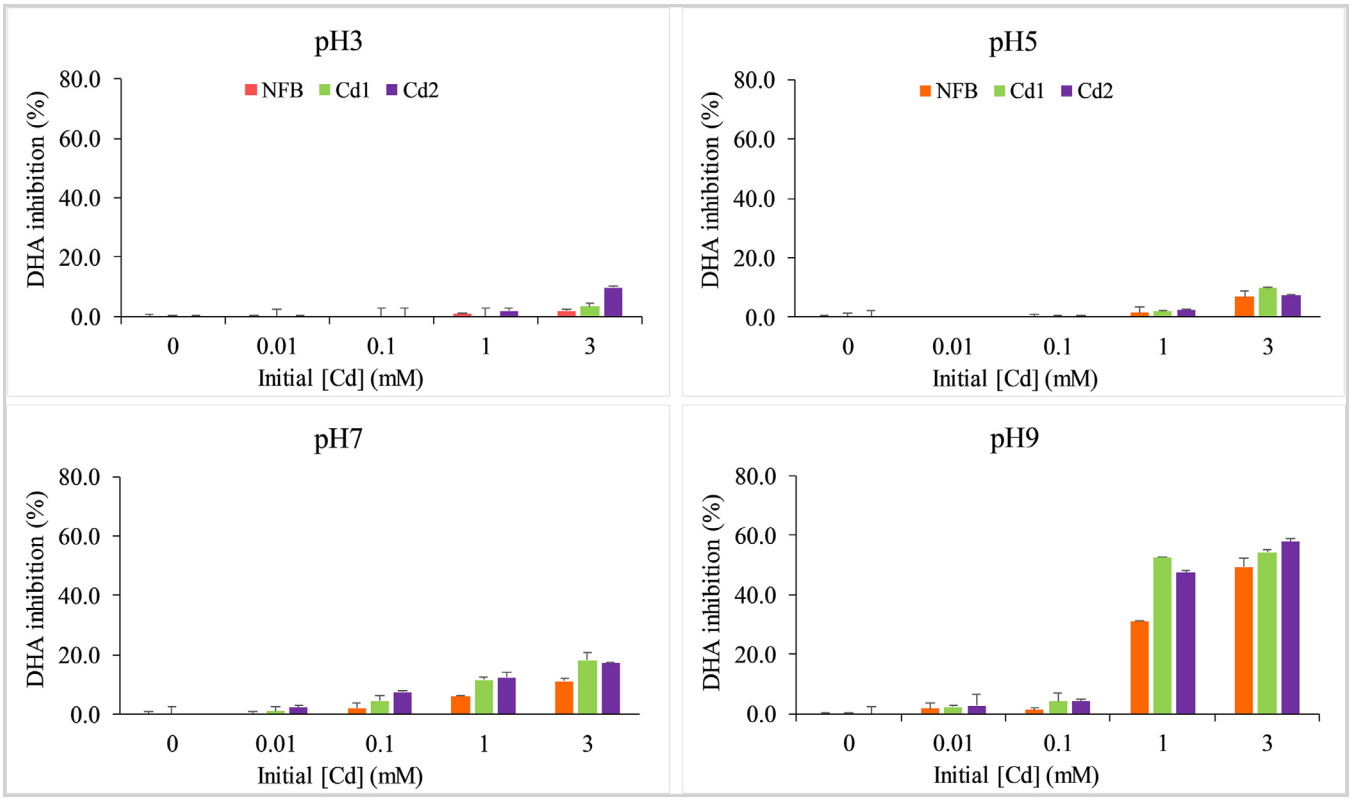

Fig. 7. Evaluation of the toxicity of Cd-unbound and Cd-bound beads. Average inhibition of *Arthrobacter globiformis* dehydrogenase activity (DHA) when subjected the bacterium to metal-bound and -unbound beads (NFB – non-functionalized beads, Cd1 and Cd2 – two types of functionalized beads) exposed to Cd solution at different initial cadmium concentrations ([Cd]) in metal-binding assays conducted at pH 3, 5, 7 and 9. Error bars represent standard deviation. The outcome of the statistical analyses performed to the data is provided in Tables S4 and S5.

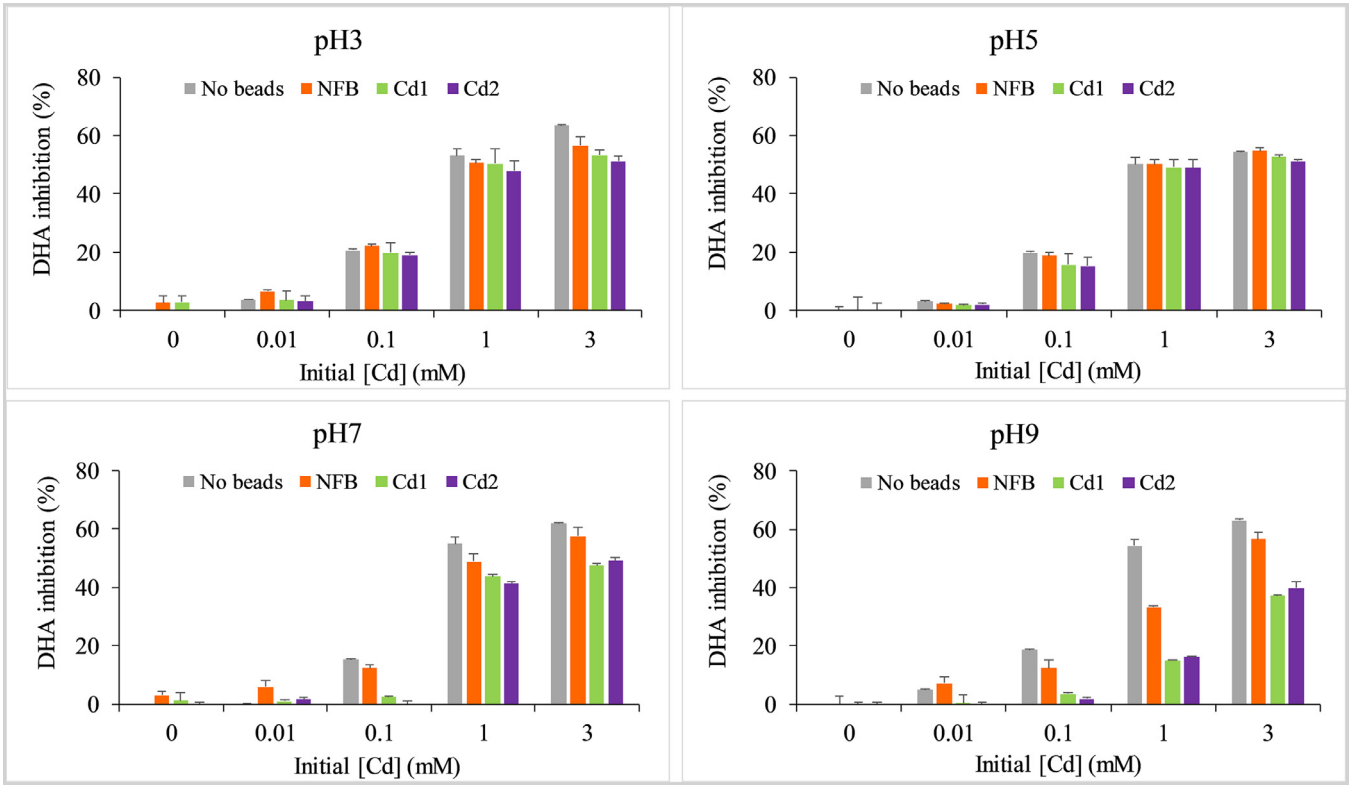

Fig. 8. Assessment of the ecotoxic potential of the remediated Cd solutions, as to evaluate the bioremediation efficiency of the beads. Average inhibition of *Arthrobacter globiformis* dehydrogenase activity (DHA) when the bacterium was subjected to Cd solutions, which were previously exposed and non-exposed to the three bead variants (NFB – non-functionalized beads, Cd1 and Cd2 – two types of functionalized beads) at pH 3, 5, 7 and 9. Error bars represent standard deviation. The outcome of the statistical analyses performed to the data is provided in Table S6.

This is coherent with the enhanced negative zeta potentials of Cd2 beads as compared to Cd1 beads at pH 7 and 9 (Fig. 4A), which resulted in the higher amount of Cd sequestered by Cd2 peptides (0.088–20.8 nmol Cd ng^{-1} peptide) relatively to the Cd1 peptides (0.009–3.8 nmol Cd ng^{-1} peptide). In turn, the zeta potentials of PHB beads at pH 5 attained the lowest values, suggesting a nearly neutral surface net charge (Fig. 4). In fact, the pI of the polar amino acids composing Cd1 and Cd2 functional peptides is ~5 (Lide, 2005), thereby explaining the lack of Cd adsorption and removal at pH 5. At acidic pH, however, the protonated carboxyl and amine groups provoke a reduction on metal removal due to electrostatic repulsive forces against the cationic Cd^{2+} (Zahri et al., 2017).

Broadly, Sips was the model that better-described Cd adsorption by functionalized beads at pH 7 and 9 (Fig. 6). Sips is normally applied to characterize metal adsorption to heterogeneous surfaces (Zahri et al., 2017). Hence, it is suggested that our beads have a heterogeneous distribution of the metal-binding sites, and that the interactions between Cd^{2+} and the functionalized beads were probably governed by a physisorption mechanism based on electrostatic attractions. This result is in agreement with the highest q values achieved under pH 9 (Fig. 5), at which beads showed pronouncedly negative zeta potentials (Fig. 4).

To build up a sustainable bioremediation loop, two important requirements should be met. First, the bioremediation agents must not be hazardous *per se* if the end-use involves their direct application into the environment. We have reached this goal since all bead types did not inhibit *A. globiformis* DHA (Fig. 7, Tables S4-S5). PHB inclusions can likely act as a carbon source fueling the energy metabolism that is mediated by DHA in bacteria (Marques et al., 2014). However, Cd-exposed beads after remediation assays were particularly toxic, inducing up to 60% DHA inhibition at increasing Cd concentrations and pH $\geq$ 7 (Fig. 7, Tables S4-S5). Therefore, *A. globiformis* response proved that the functionalized beads had retained Cd and, as a consequence, the toxicity of Cd-exposed beads demands cautious confinement of the bioremediation process for *in situ* applications.

The second requirement is that the selected techniques and agents should guarantee effective bioremediation, which is usually assessed by a framework that combines chemical and ecotoxicological analyses. The chemical counterpart confirmed the successful removal of Cd loads (Fig. 5, Tables S2-S3). Likewise, the toxicity of remediated Cd solutions was drastically reduced as indicated by the reduced inhibition of *A. globiformis* DHA, notably at initial Cd concentrations below 0.1 mM (pH 7) and 1 mM (pH 9) (Fig. 8). The tested range of Cd concentrations was based on the Cd levels detected in aqueous samples from mine areas (*e.g.,*Neiva et al., 2014), as well as it had into consideration potential worst-case scenarios of Cd contamination. Hence, at environmentally significant Cd concentrations (0.01 mM), Cd1 and Cd2 beads had also promoted Cd removal (1.3% and 3.0% at pH 3, 23.8 and 39.2% at pH 7, 51.4 and 47.1% at pH9, respectively for Cd1 and Cd2 beads) and toxicity reduction. It is thereby strengthened the relevance and efficiency of the functionalized beads for potential environmental applications towards Cd cleansing.

5. Conclusion

We have accomplished the proof of concept in that new bio-based PHB materials were designed and manufactured by engineered *E. coli* for effective Cd bioremediation. In particular, the Cd-binding peptide fused to the C-terminus of the PhaC protein (*i.e.,* Cd1 beads) retained PhaC-PHB-bead-forming function, resulting in higher production yields and Cd bioremediation performance than the Cd-binding peptide fused to the N-terminus of the PhaC protein (*i.e.,* Cd2 beads) and only PhaC protein without the Cd-binding peptide (*i.e.,* NFB beads). These innovative bioremediation agents offer additional valuable advantages since they can be synthesized and functionalized in one step in engineered bacteria through a cost-effective process ready for scale-up, are biodegradable and completely out of the prohibiting regulations on the release of GMOs. Moreover, the beads can maintain their stability and functionality under acidic or alkaline pH, which are constraining factors for successful bioremediation of metal-contaminated matrices (*e.g.,* acid mine drainage effluents and alkaline treatment ponds of mine tailings) (Carvalho, 2017). Therefore, this is a groundbreaking innovation in the bioremediation arena, chiefly because our platform can be further improved and/or customized to target the future reclamation of other metal contaminants.

Supporting Information: Supporting Information is available.

Declaration of Competing Interest

The authors declare that they have no known competing financial interests or personal relationships that could have appeared to influence the work reported in this paper.

Acknowledgments

We acknowledged the financial support for CESAM (UIDP/50017/2020+UIDB/50017/2020) and CICECO-Aveiro Institute of Materials (UIDB/50011/2020+UIDP/50011/2020) to FCT/MEC, through national funds. This work was also funded by the Portuguese Foundation for Science and Technology (FCT) and by the European Regional Development Fund (ERDF) through the Portugal 2020 Partnership Agreement between Portugal and the European Union, the Competitiveness and Internationalization Operational Programme (COMPETE 2020) and the Regional Operational Programme Lisboa (POR-Lisboa), under the project NANOBINDERS (PTDC/AAG-REC/3004/2014). Catarina R. Marques is funded by national funds (OE), through FCT – Fundação para a Ciência e a Tecnologia, I.P., in the scope of the framework contract foreseen in the numbers 4, 5 and 6 of the article 23, of the Decree-Law 57/2016, of August 29, changed by Law 57/2017 of July 19. We are grateful for funding received from Griffith University (Australia) as part of the Griffith 2020 strategy. The authors also wish to thank François Baneyx (University of Washington, USA) for his assistance in identifying suitable Cd binding peptides.

Supplementary materials

Supplementary material associated with this article can be found, in the online version, at doi:10.1016/j.watres.2020.116357.

References

Alho, L., de, O.G., Gebara, R.C., Paina, K., de, A., Sarmento, H., Melão, M., da, G.G., 2019. Responses of *Raphidocelis subcapitata* exposed to Cd and Pb: mechanisms of toxicity assessed by multiple endpoints. Ecotox. Environ. Saf. 169, 950–959. https://doi.org/10.1016/j.ecoenv.2018.11.087.

Amara, A.A., Rehm, B.H.A., 2003. Replacement of the catalytic nucleophile cysteine-296 by serine in class II polyhydroxyalkanoate synthase from Pseudomonas aeruginosa-mediated synthesis of a new polyester: identification of catalytic residues. Biochem. J. 374, 413–421. https://doi.org/10.1042/bj20030431.

Bae, W., Chen, W., Mulchandani, A., Mehra, R.K., 2000. Enhanced bioaccumulation of heavy metals by bacterial cells with surface-displayed synthetic phytochelatins. Biotechnol Bioeng 411–418. https://doi.org/10.1021/bk-2002-0806.ch024.

Blatchford, P.A., Scott, C., French, N., Rehm, B.H.A., 2012. Immobilization of organophosphohydrolase OpdA from *Agrobacterium radiobacter* by overproduction at the surface of polyester inclusions inside engineered *Escherichia coli*. Biotechnol. Bioeng. 109, 1101–1108. https://doi.org/10.1002/bit.24402.

Blindauer, C.A., 2011. Bacterial metallothioneins: past, present, and questions for the future. J. Biol. Inorg. Chem. 16, 1011–1024. https://doi.org/10.1007/s00775-011-0790-y.

Burakov, A.E., Galunin, E.V., Burakova, I.V., Kucherova, A.E., Agarwal, S., Tkachev, A.G., Gupta, V.K., 2018. Adsorption of heavy metals on conventional and nanostructured materials for wastewater treatment purposes: a review. Ecotox. Environ. Saf. 148, 702–712. https://doi.org/10.1016/j.ecoenv.2017.11.034.

Carvalho, F.P., 2017. Mining industry and sustainable development: time for change. Food Energy Secur. 61–77. https://doi.org/10.1002/fes3.109.
Copello, G.J., Varela, F., Vivot, R.M., Díaz, L.E., 2008. Immobilized chitosan as biosorbent for the removal of Cd(II), Cr(III) and Cr(VI) from aqueous solutions. Bioresour. Technol. 99, 6538–6544. https://doi.org/10.1016/j.biortech.2007.11.055.
Eskandari, V., Yakhchali, B., Sadeghi, M., Karkhane, A.A., 2013. *In silico* design and construction of metal-binding hybrid proteins for specific removal of cadmium based on CS3 pili display on the surface of *Escherichia coli*. Biotechnol. Appl. Biochem. 60, 564–572. https://doi.org/10.1002/bab.1132.
European Comission, 2008. Directive 2008/105/EC of the European Parliament and of the Council of 16 December 2008 on environmental quality standards in the field of water policy. Off. J. European Union.
Flynn, C.E., Mao, C., Hayhurst, A., Williams, J.L., Georgiou, G., Iverson, B., Belcher, A.M., 2003. Synthesis and organization of nanoscale II-VI semiconductor materials using evolved peptide specificity and viral capsid assembly. J. Mater. Chem. 13, 2414–2421. https://doi.org/10.1039/b307593a.
González-Miró, M., Rodríguez-Noda, L.M., Fariñas-Medina, M., Cedré-Marrero, B., Madariaga-Zarza, S., Zayas-Vignier, C., Hernández-Cedeño, M., Kleffmann, T., García-Rivera, D., Vérez-Bencomo, V., Rehm, B.H.A., 2018. Bioengineered polyester beads co-displaying protein and carbohydrate-based antigens induce protective immunity against bacterial infection. Sci. Rep. 8, 1–15. https://doi.org/10.1038/s41598-018-20205-7.
Hay, I.D., Hooks, D.O., Rehm, B.H.A., 2017. Use of Bacterial Polyhydroxyalkanoates in Protein Display Technologies. In: McGenity, T.J., Timmis, K.N., Nogales, B. (Eds.), Hydrocarbon and Lipid Microbiology Protocols. Springer Protocols Handbooks, Berlin Heilderberg, pp. 71–86.
He, X., Chen, W., Huang, Q., 2012. Surface display of monkey metallothionein α tandem repeats and EGFP fusion protein on *Pseudomonas putida* X4 for biosorption and detection of cadmium. Appl. Microbiol. Biotechnol. 95, 1605–1613. https://doi.org/10.1007/s00253-011-3768-3.
Hooks, D.O., Venning-Slater, M., Du, J., Rehm, B.H.A., 2014. Polyhydroyxalkanoate synthase fusions as a strategy for oriented enzyme immobilisation. Molecules 19, 8629–8643. https://doi.org/10.3390/molecules19068629.
Huang, Z., Chen, G., Zeng, G., Chen, A., Zuo, Y., Guo, Z., Tan, Q., Song, Z., Niu, Q., 2015. Polyvinyl alcohol-immobilized *Phanerochaete chrysosporium* and its application in the bioremediation of composite-polluted wastewater. J. Hazard. Mater. 289, 174–183. https://doi.org/10.1016/j.jhazmat.2015.02.043.
Jahns, A.C., Rehm, B.H.A., 2012. Relevant uses of surface proteins - display on self-organized biological structures. Microb. Biotechnol. 5, 188–202. https://doi.org/10.1111/j.1751-7915.2011.00293.x.
ISO (International Organization for Standardization), 2016. ISO 18187/2016 - Soil quality — Contact test for solid samples using the dehydrogenase activity of *Arthrobacter globiformis*. ISO (International Organization for Standardization), Geneve, Switzerland.
Jahns, A.C., Rehm, B.H.A., 2009. Tolerance of the *Ralstonia eutropha* class I polyhydroxyalkanoate synthase for translational fusions to its C terminus reveals a new mode of functional display. Appl. Environ. Microbiol. 75, 5461–5466. https://doi.org/10.1128/AEM.01072-09.
Khairy, M., El-Safty, S.A., Shenashen, M.A., 2014. Environmental remediation and monitoring of cadmium. TrAC - Trends Anal. Chem. 62, 56–68. https://doi.org/10.1016/j.trac.2014.06.013.
Li, P.S., Tao, H.C., 2015. Cell surface engineering of microorganisms towards adsorption of heavy metals. Crit. Rev. Microbiol. 41, 140–149. https://doi.org/10.3109/1040841X.2013.813898.
Li, Z., Katsumi, T., Imaizumi, S., Tang, X., Inui, T., 2010. Cd(II) adsorption on various adsorbents obtained from charred biomaterials. J. Hazard. Mater. 183, 410–420. https://doi.org/10.1016/j.jhazmat.2010.07.040.
Lide, D.R., et al., 2005. Handbook of Chemistry and Physics, 85th ed CRC Press, Boca Raton, FL.
Liu, L., Bilal, M., Duan, X., Iqbal, H.M.N., 2019. Mitigation of environmental pollution by genetically engineered bacteria — Current challenges and future perspectives. Sci. Total Environ. 667, 444–454. https://doi.org/10.1016/j.scitotenv.2019.02.390.
Marques, C.R., 2016. Bio-rescue of marine environments: on the track of microbially-based metal/metalloid remediation. Sci. Total Environ. 565, 165–180. https://doi.org/10.1016/j.scitotenv.2016.04.119.
Marques, C.R., Caetano, A.L., Haller, A., Gonc, F., Pereira, R., Römbke, J., 2014. Toxicity screening of soils from different mine areas — A contribution to track the sensitivity and variability of *Arthrobacter globiformis* assay. J. Hazard. Mater. 274, 331–341. https://doi.org/10.1016/j.jhazmat.2014.03.066.
Marques, C.R., El-azhari, N., Martin-laurent, F., Pandard, P., Meline, C., Petre, A.L., Eckert, S., Zipperle, J., Vá, M., Maly, S., Lucie, Š., Slavíková, A., Hofman, J., Kumar, A., Doan, H., Mclaughlin, M., Richter, E., Römbke, J., 2018. A bacterium-based contact assay for evaluating the quality of solid samples – Results from an international ring-test. J. Hazard. Mater. 352, 139–147. https://doi.org/10.1016/j.jhazmat.2018.03.022.
Martinis, E.M., Olsina, R.A., Altamirano, J.C., Wuilloud, R.G., 2009. On-line ionic liquid-based preconcentration system coupled to flame atomic absorption spectrometry for trace cadmium determination in plastic food packaging materials. Talanta 78, 857–862. https://doi.org/10.1016/j.talanta.2008.12.051.
Martins, M.C., Santos, E.B.H., Marques, C.R., 2017. First study on oyster-shell-based phosphorous removal in saltwater — A proxy to effluent bioremediation of marine aquaculture. Sci. Total Environ. 574, 605–615. https://doi.org/10.1016/j.scitotenv.2016.09.103.
Mejàre, M., Ljung, S., Bulow, L., 1998. Selection of cadmium specific hexapeptides and their expression as OmpA fusion proteins in *Escherichia coli*. Protein Eng. Des. Sel. 11, 489–494. https://doi.org/10.1093/protein/11.6.489.
Moradali, M.F., Rehm, B.H.A., 2020. Bacterial biopolymers: from pathogenesis to advanced materials. Nat. Rev. Microbiol. 18, 195–210.
Mudhoo, A., Garg, V.K., Wang, S., 2012. Removal of heavy metals by biosorption. Environ. Chem. Lett. 10, 109–117. https://doi.org/10.1007/s10311-011-0342-2.
Mueller, N.D., Gerber, J.S., Johnston, M., Ray, D.K., Ramankutty, N., Foley, J.A., 2012. Closing yield gaps through nutrient and water management. Nature.. https://doi.org/10.1038/nature11420.
Neiva, A.M.R., Carvalho, P.C.S., Antunes, I.M.H.R., Silva, M.M.V.G., Santos, A.C.T., Pinto, M.M.S.C., Cunha, P.P., 2014. Contaminated water, stream sediments and soils close to the abandoned Pinhal do Souto uranium mine, central Portugal. J. Geochemical Explor. 136, 102–117. https://doi.org/10.1016/j.gexplo.2013.10.014.
Nguyen, T.A.H., Ngo, H.H., Guo, W.S., Zhang, J., Liang, S., Yue, Q.Y., Li, Q., Nguyen, T.V., 2013. Applicability of agricultural waste and by-products for adsorptive removal of heavy metals from wastewater. Bioresour. Technol. 148, 574–585. https://doi.org/10.1016/j.biortech.2013.08.124.
Ogura, K., Rehm, B.H.A., 2019. Alginate encapsulation of bioengineered protein-coated polyhydroxybutyrate particles: a new platform for multifunctional composite materials. Adv. Funct. Mater. 29, 1–17. https://doi.org/10.1002/adfm.201901893.
Oliveira, F.C., Dias, M.L., Castilho, L.R., Freire, D.M.G., 2007. Characterization of poly(3-hydroxybutyrate) produced by *Cupriavidus necator* in solid-state fermentation. Bioresour. Technol. 98, 633–638. https://doi.org/10.1016/j.biortech.2006.02.022.
Pandey, J., Chauhan, A., Jain, R.K., 2009. Integrative approaches for assessing the ecological sustainability of *in situ* bioremediation. FEMS Microbiol. Rev. 33, 324–375. https://doi.org/10.1111/j.1574-6976.2008.00133.x.
Parlane, N.A., Gupta, S.K., Rubio-Reyes, P., Chen, S., Gonzalez-Miro, M., Wedlock, D.N., Rehm, B.H.A., 2017. Self-assembled protein-coated polyhydroxyalkanoate beads: properties and biomedical applications. ACS Biomater. Sci. Eng. 3, 3043–3057. https://doi.org/10.1021/acsbiomaterials.6b00355.
Quinn, G., Keough, M., 2002. Experimental Design and Data Analysis For Biologists. University Press, Cambridge.
Rehm, B.H.A., 2010. Bacterial polymers: biosynthesis, modifications and applications. Nat. Rev. Microbiol. 8, 578–592. https://doi.org/10.1038/nrmicro2354.
Robins, K.J., Hooks, D.O., Rehm, B.H.A., Ackerley, D.F., 2013. *Escherichia coli* Nema is an efficient chromate reductase that can be biologically immobilized to provide a cell free system for remediation of hexavalent chromium. PLoS ONE 8. https://doi.org/10.1371/journal.pone.0059200.
Rubio Reyes, P., Parlane, N.A., Wedlock, D.N., Rehm, B.H.A., 2016. Immunogencity of antigens from *Mycobacterium tuberculosis* self-assembled as particulate vaccines. Int. J. Med. Microbiol. 306, 624–632. https://doi.org/10.1016/j.ijmm.2016.10.002.
Schaider, L.A., Senn, D.B., Estes, E.R., Brabander, D.J., Shine, J.P., 2014. Sources and fates of heavy metals in a mining-impacted stream: temporal variability and the role of iron oxides. Sci. Total Environ. 490, 456–466. https://doi.org/10.1016/j.scitotenv.2014.04.126.
Sousa, C., Kotrba, P., Ruml, T., Cebolla, A., De Lorenzo, V., 1998. Metalloadsorption by *Escherichia coli* cells displaying yeast and mammalian metallothioneins anchored to the outer membrane protein LamB. J. Bacteriol. 180, 2280–2284.
Suresh Kumar, K., Dahms, H.U., Won, E.J., Lee, J.S., Shin, K.H., 2015. Microalgae - A promising tool for heavy metal remediation. Ecotoxicol. Environ. Saf. 113, 329–352. https://doi.org/10.1016/j.ecoenv.2014.12.019.
Tilman, D., Balzer, C., Hill, J., Befort, B.L., 2011. Global food demand and the sustainable intensification of agriculture. PNAS 108. https://doi.org/10.1073/pnas.1116437108
Urgun-Demirtas, M., Stark, B., Pagilla, K., 2006. Use of genetically engineered microorganisms (GEMs) for the bioremediation of contaminants. Crit. Rev. Biotechnol. 26, 145–164. https://doi.org/10.1080/07388550600842794.
Vinod, V.T.P., Sashidhar, R.B., Sreedhar, B., Rama Rao, B., Nageswara Rao, T., Abraham, J.T., 2009. Interaction of Pb2+ and Cd2+ with gum kondagogu (*Cochlospermum gossypium*): a natural carbohydrate polymer with biosorbent properties. Carbohydr. Polym. 78, 894–901. https://doi.org/10.1016/j.carbpol.2009.07.025.
Williams, P., Lei, M., Sun, G., Huang, Q., Lu, Y., Deacon, C., Meharg, A., Zhu, Y., 2009. Occurrence and partitioning of cadmium, arsenic and lead in mine impacted paddy rice: hunan. China. Environ. Sci. Technol. 43, 637–642.
Xu, Z., Lee, S.Y., 1999. Display of polyhistidine peptides on the *Escherichia coli* cell surface by using outer membrane protein C as an anchoring motif. Appl. Environ. Microbiol. 65, 5142–5147.
Yee, L., Blanch, H., 1992. Recombinant Protein Expression in High Cell Density Fed–Batch Cultures of *Escherichia coli*. Nat. Biotechnol. 10, 1550–1556.
Zahri, N.A.M., Jamil, S.N.A.M., Abdullah, L.C., Jia Huey, S., Yaw, T.C.S., Mobarekeh, M.N., Rapeia, N.S.M., 2017. Equilibrium and kinetic behavior on cadmium and lead removal by using synthetic polymer. J. Water Process Eng. 17, 277–289. https://doi.org/10.1016/j.jwpe.2017.04.013.
Zamil, S.S., Choi, M.H., Song, J.H., Park, H., Xu, J., Chi, K.W., Yoon, S.C., 2008. Enhanced biosorption of mercury(II) and cadmium(II) by cold-induced hydrophobic exobiopolymer secreted from the psychrotroph *Pseudomonas fluorescens* BM07. Appl. Microbiol. Biotechnol. 80, 531–544. https://doi.org/10.1007/s00253-008-1621-0.
Zhou, W., Liu, D., Zhang, H., Kong, W., Zhang, Y., 2014. Bioremoval and recovery of Cd(II) by *Pseudoalteromonas* sp. SCSE709-6: comparative study on growing and grown cells. Bioresour. Technol. 165, 145–151. https://doi.org/10.1016/j.biortech.2014.01.119.